

# Heavy Metal and Hydrocarbon Pollution in Recent Sediments from Southampton Water, Southern England: A Geochemical and Isotopic Study

IAN W. CROUDACE\* AND  
ANDREW B. CUNDY†

*Department of Geology, University of Southampton,  
Southampton SO17 1BJ, U.K.*

A sediment core from Southampton Water, a coastal plain estuary, has been investigated and is shown to provide a record of pollution following the expansion of the Fawley oil refinery in 1949-1951. A combination of heavy metal analyses, the first appearance of hydrocarbon contamination, radiometric dating, and stable Pb isotope ratios have been used to interpret the pollution history in the core. Indications are that following dredging activities, accompanying the refinery expansion, there was a relatively rapid sedimentation rate of *ca.* 20 mm p.a., which decreased with time to approximately 5 mm p.a. The higher accumulation rate is attributed to the response of the estuary following the major capital dredging works that occurred in 1950-1951. The accumulation rates are used to recalculate concentration profiles to reveal the heavy metal flux to the sediments. Lead isotope data indicate a significant post-1950 use of lead derived from ancient, non-U.K. (Precambrian) ores in local industry.

## Introduction

Southampton Water is a coastal plain estuary (1) forming a northwesterly extension to the central Solent (Figure 1). It is an approximately rectangular body of water (10 km long by 2 km wide), receiving freshwater input principally from the Rivers Test and Itchen at its head, although these contribute only a small fraction to the tidal prism. The substrate within Southampton Water is generally mud or sandy mud that is often rich in organic matter, and extensive salt marshes have developed along its western flank. Southampton Water is well-known for having a remarkable tidal regime caused by a combination of the geometry of the English Channel, the Cherbourg Peninsula, and the two entrances to the Solent around the Isle of Wight (2). These lead to a useful hydrographic property of a double high water stand covering nearly 2 h. The NW-SE orientation of Southampton Water protects it from powerful waves generated from the prevailing southwesterly winds. Capital dredging programs were made in the estuary and its western approaches around the turn of the century, between the two World Wars, in 1950, and in 1962 (2). The bed of the estuary requires little maintenance dredging because of its stable Tertiary clay substrate and the protection of the estuary from heavy seas. These facts make Southampton Water very attractive to high-tonnage shipping.

The areas around Southampton Water have undergone significant industrial, residential, and leisure development, particularly during the last 50 years. Major sources of effluent discharge into Southampton Water are shown in Figure 1. Of note is the intensive use of the western shore area with the large scale Esso oil refinery at Fawley and the development of related industries that use the feedstock from the refinery. The Fawley refinery is the largest in the United Kingdom, handling over 20 Mt of crude oil per year, and is one of the most complex in Europe (4, 5). Operations started in 1921 (the AGWI plant, Atlantic Gulf West Indies Corp.), and in the early 1950s it was developed and enlarged significantly by Esso. A steam-cracking process is used in which water comes in contact with oil, and the effluent inevitably has hydrocarbon contamination. An estimated  $18 \times 10^6$  L/h of water is abstracted from Southampton Water for various processes, most of which is returned through outfalls. Throughout the last 40 years, the plant is known to have been a major contributor of hydrocarbon pollution in Southampton Water (6-8) although effluent quality improvements over the last two decades have led to marked reductions in these discharges. For example, since 1970 the oil content of the wastewater has fallen from more than 30 ppm to less than 3 ppm (7). Copper is used in several processes within the refinery, some of which ends up in the waste stream. Knap (4) reported that copper is used as a catalyst to convert mercaptans to disulfides. Additionally, cuprous ammonium acetate has been used to remove acetylene gas. The discharge pattern of copper is not known in detail, and it is probable that it is continuously output with an occasional spike (see ref 8). Lead is probably

\* Present address: Neotectonics Research Unit, Department of Geography, Brunel University College, Lancaster House, Borough Road, London TW7 5DU, U.K.

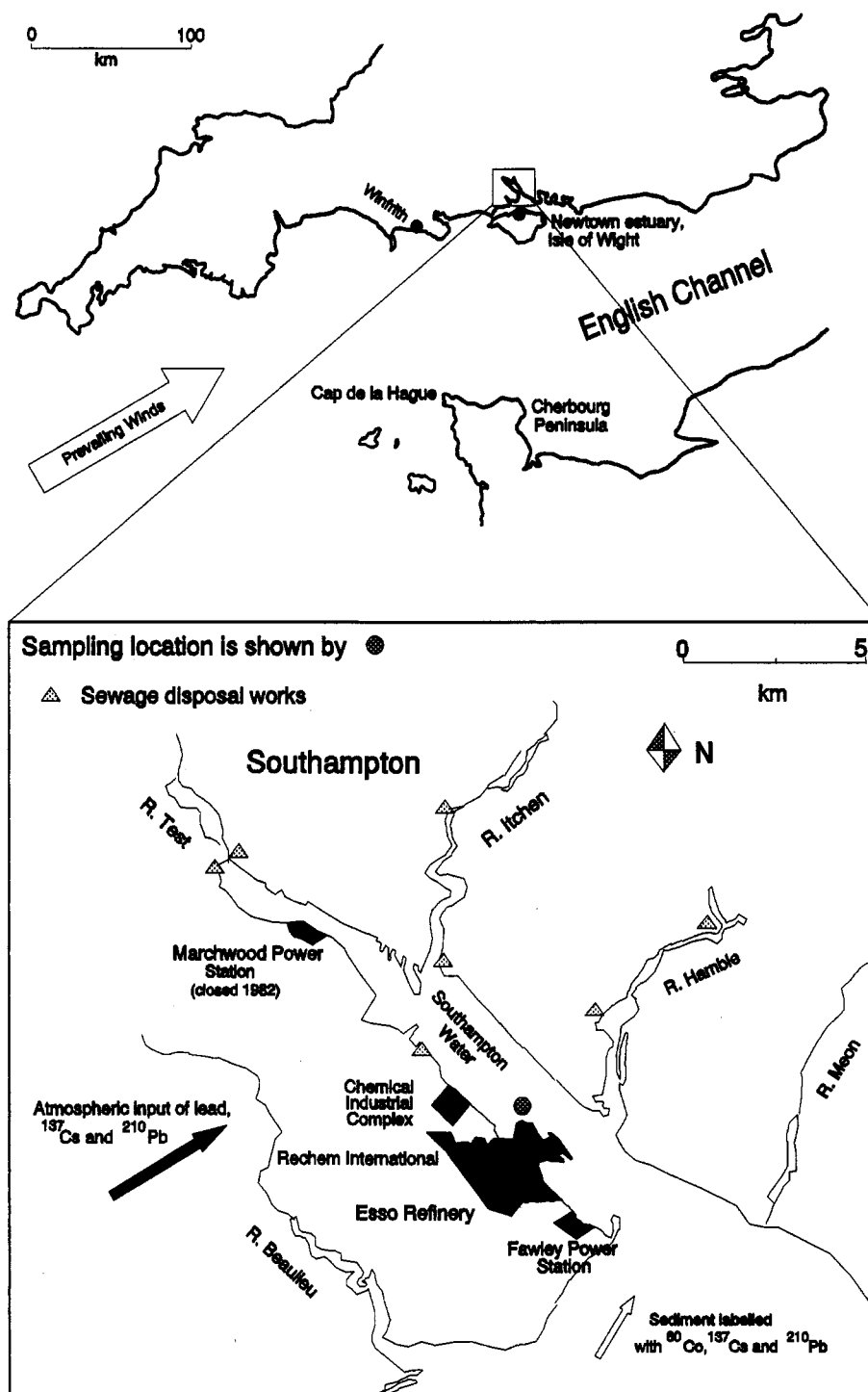


**FIGURE 1.** Study area—Southampton Water (Southern England). Major sources of effluent discharge are also shown [after Webber (3) and Cundy (10)].

discharged from one or more companies, but the concentrations are considerably lower than those found for copper. The present study, part of a broader investigation into estuarine accumulation rates and sediment geochemistry, examines the effects of this industrialization on the sedimentation regime and the trace element contamination of sediments from the Fawley area of Southampton Water. Discharge products, in part from Fawley, are used in combination with radiochronology (using  $^{137}\text{Cs}$ ,  $^{60}\text{Co}$ , and  $^{210}\text{Pb}_{\text{xs}}$ ) to determine sediment accumulation rates. An investigation of lead isotope ratios allows general inferences to be drawn on the sources of the Pb.

## Methodologies

A gravity core was taken from a subtidal area near the main outfall (approximately 200 m from outfall no. 1) of the Esso oil refinery (sampling location shown in Figure 1) in March 1989. The core was collected by boat during low tide on the margin of the main navigation channel from a water depth of approximately 10 m. The core, 70 cm  $\times$  7 cm o.d., was split, logged, and divided into 3-cm subsamples for analysis. In retrospect, it would have been better to have sampled at 1-cm intervals to improve the resolution of the observations.

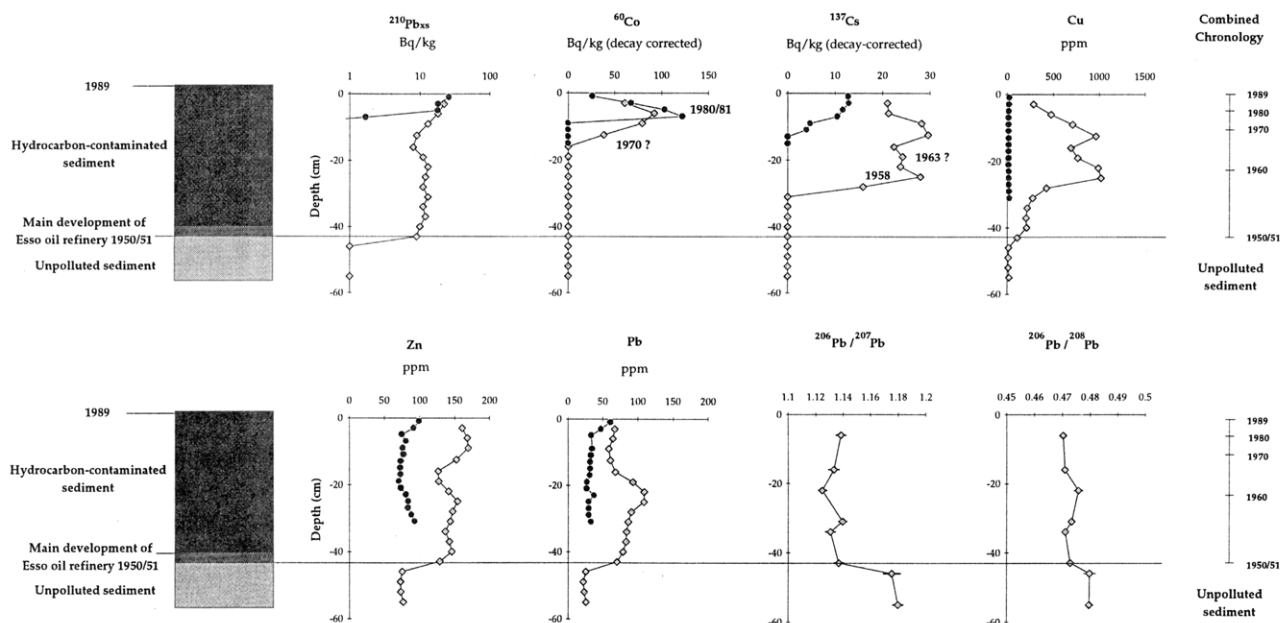


**FIGURE 2.** Sedimentary log,  $^{210}\text{Pb}_{\text{xs}}$ ,  $^{60}\text{Co}$ ,  $^{137}\text{Cs}$ , Cu, Zn, Pb, and Pb isotope ratios versus depth for the Fawley subtidal core. Data from the Newtown intertidal core (relatively unpolluted), where available, are shown by the solid circles for comparison.

$^{210}\text{Pb}$  activity was determined through the measurement of its granddaughter  $^{210}\text{Po}$  using  $\alpha$ -spectrometry (proxy method). The method employed is based on ref 9 and uses double acid leaching of the sediment and autodeposition of the Po in the leachate onto silver disks. The supported  $^{210}\text{Pb}$  activity was obtained using  $^{214}\text{Pb}$  and  $^{214}\text{Bi}$  determined from  $\gamma$ -spectrometry.  $^{209}\text{Po}$  was used as an isotopic tracer to determine sample activities.  $^{137}\text{Cs}$  and  $^{60}\text{Co}$  activities were determined by  $\gamma$ -spectrometry (using a Canberra 30% P-type HPGe detector). Detection limits are 0.5 Bq/kg for  $^{137}\text{Cs}$  and  $^{60}\text{Co}$  and 1 Bq/kg for  $^{210}\text{Pb}$ . All samples were pelletized for trace elements, fused for major element determinations, and analyzed using X-ray fluorescence on a Philips PW1400 sequential X-ray spectrometer system to obtain geochemical concentration data. The errors for major element data are smaller than 2% relative, and those for trace elements are smaller than 5% relative.

Lead isotopic abundances were determined using a Fisons Elemental PQ2 inductively-coupled plasma mass spectrometer (ICP/MS). Full details of the chemical methodology and analysis conditions are given in Cundy (10), but essentially samples were acid leached and the Pb was preconcentrated on Dowex 1-X8 200–400 columns using 0.5 M HBr. A hydrocarbon extract was also taken from a sample in the middle of the core to determine its isotopic character. The Pb level, however, was too low to make any measurements. Mass fractionation corrections were applied to the isotopic data. Errors on the isotopic ratios are shown as bars in the plotted data (see Figure 2) and are better than 0.5% for  $^{206}\text{Pb}/^{207}\text{Pb}$  and  $^{206}\text{Pb}/^{208}\text{Pb}$  and better than 0.8% for  $^{206}\text{Pb}/^{204}\text{Pb}$ . NIST 981 (a natural Pb ore reference material) was measured to assess accuracy, and sample blanks were also run to determine possible contamination.

## Results and Discussion

**Chronology. (A) Sedimentary Log.** The sedimentary log (Figure 2) for the core examined shows a number of important features. The upper 40 cm of the core is almost black, partly caused through the obvious presence of hydrocarbons [also observed by Ármannsson (11) in sedi-

ments from this locality]. The peak hydrocarbon content of the contaminated zone is approximately 2 wt %. The sediment is muddy and has no visible sedimentary structures. Between 40.0 and 42.5 cm depth, there is a transitional zone of dark gray muddy sediment below which there is a more compacted gray-green sediment which is free of hydrocarbon contamination. This lowermost gray-green zone represents unpolluted Holocene sediment and is considered to lie below an excavation surface (see later). It is notable that the Holocene sediments are derived mostly through the erosion of Tertiary coastal strata exposed west of Southampton Water and from riverine inputs (also weathering of similar Tertiary bedrock). The source of hydrocarbons in the core is either from tankers unloading at the Esso refinery or from the refinery itself. It is well-known from various studies (7) that hydrocarbons are introduced into Southampton Water and that clear environmental damage to local salt marshes has resulted, especially during the early years of the refinery's operation. Discharges of effluent began following the refinery's large-scale expansion in 1949–1951 (4). The clear nature of the boundary between the oil-contaminated sediment and the underlying sediment is due to the lack of bioturbation in the recently excavated unpolluted muds. This boundary provides an effective marker horizon in the sediment column; approximately 43 cm of sediment accumulated during the period 1950/1951–1989, which gives an average sediment accumulation rate of 11 mm p.a. (Table 1).

**(B)  $^{210}\text{Pb}_{\text{xs}}$  (Half-Life 22 Years) Dating.**  $^{210}\text{Pb}$  is a naturally occurring radionuclide formed as a product of the  $^{238}\text{U}$  decay series.  $^{226}\text{Ra}$  in soils and crustal rocks decays to  $^{222}\text{Rn}$ , a noble gas. A fraction of the  $^{222}\text{Rn}$  that is produced escapes to the atmosphere where it decays through a series of short-lived daughters to  $^{210}\text{Pb}$ .  $^{210}\text{Pb}$  is rapidly removed from the atmosphere by precipitation and is incorporated in accumulating sediment. This is termed the unsupported or excess activity ( $^{210}\text{Pb}_{\text{xs}}$ ). The total  $^{210}\text{Pb}$  measured is the sum of this excess activity and the so-called "supported" activity resulting from the decay of  $^{226}\text{Ra}$  in the sediment itself. Once incorporated into the sediment,  $^{210}\text{Pb}_{\text{xs}}$  will

TABLE 1

Average Sediment Accumulation Rates with Time for the Fawley Sediment Core<sup>a</sup>

dating method	possible sources	period	av accumulation rate over period (mm p.a.)
presence of hydrocarbon effluent	Esso oil refinery and local industry	1950–1989	11
elevated Cu concns	Esso oil refinery and local industry	1950–1989	11
<sup>210</sup> Pb <sub>XS</sub>	naturally produced	1950–ca. 1964	20
		ca. 1964–1989	5
<sup>137</sup> Cs	atomic weapons testing	1958–1989	7–9 <sup>b</sup>
<sup>60</sup> Co	neutron activation product, AEE Winfrith reactor	1980–1989	6

<sup>a</sup> Values shown are to the nearest mm to allow for errors caused by the sampling interval. <sup>b</sup> From flux data. <sup>c</sup> Maximum.

decay at a known rate, allowing the estimation of sediment accumulation rates through the measurement of <sup>210</sup>Pb<sub>XS</sub> activity (ref 14). Inflections in the <sup>210</sup>Pb<sub>XS</sub> profile mark changes in accumulation rate or are due to bioturbation. Rates are calculated in the present study using the "simple" model or constant flux: constant sedimentation rate model (15).

<sup>210</sup>Pb<sub>XS</sub> activity vs depth for the core examined is shown in Figure 2. The profile may be divided into three main sections:

(a) surface–16 cm depth, where the gradient gives a sediment accumulation rate of 5 mm p.a.

(b) 22–43 cm depth, where the gradient gives an accumulation rate of ca. 20 mm p.a.

(c) 43 cm–core base, where no excess <sup>210</sup>Pb activity is present and the measured <sup>210</sup>Pb activity is due to the decay of <sup>226</sup>Ra.

The data show a clear pattern of a decreasing sediment accumulation rate with time. Higher rates occurred immediately after the expansion of the refinery (Table 1) in 1949–1951. The sharp drop in <sup>210</sup>Pb<sub>XS</sub> to zero below 43 cm is consistent with the removal of a portion of the Holocene mud, thereby exposing older pre/early Industrial Holocene sediment. This was most probably caused through dredging. At first, it was considered that this gray-green clay at the base of the core was Tertiary in age. Tertiary clays lie beneath the Holocene muds in Southampton Water and could easily have been exposed following the capital dredging program that occurred around 1950. An examination of foraminifera from this material, however, showed the fauna to be Holocene (J. W. Murray, personal communication).

(C) <sup>60</sup>Co (Half-Life 5 Years) Dating. The second artificial radionuclide examined in the study is <sup>60</sup>Co, a neutron activation product originating from the prototype steam generating heavy water reactor at AEE Winfrith, Dorset. Authorized discharges of treated effluent were made to sea between 1970 and 1990, when the reactor was closed (13). Sediments in the area surrounding the discharge pipeline have been labeled with <sup>60</sup>Co, and this "spiked" material is transported eastward into the Solent and Southampton Water. The maximum discharge of <sup>60</sup>Co occurred in 1980/1981, providing a peak in activity in local marine sediments that may be used to derive rates of sediment accumulation (10). An accurate sedimentation rate is difficult to obtain from the decay-corrected activity–depth profile shown in Figure 2 due to the large sampling interval. A maximum in activity at 6 cm depth corresponds to 1980/1981 and gives a maximum sediment accumulation rate of 6 mm p.a. A second estimate of sediment accumulation rate may be obtained from the greatest depth at which <sup>60</sup>Co can be detected, which should correspond to 1970, the starting

year of discharge. This gives a maximum sediment accumulation rate of 5.5 mm p.a., but this could be unreliable if diffusive processes (via redox changes) caused downward movement of <sup>60</sup>Co.

(D) <sup>137</sup>Cs (Half-Life 30 Years) Dating. <sup>137</sup>Cs is present in the study area due to atmospheric fallout from nuclear weapons testing and reactor accidents. Marked maxima in deposition of <sup>137</sup>Cs occurred in 1958, in 1963 (both due to above ground nuclear testing), and to a lesser extent in Southern England in 1986 (from the Chernobyl incident). These provide profile spikes in recent sediment that can be used to obtain rates of sediment accumulation. Full details of the <sup>137</sup>Cs dating method are given by Ritchie and McHenry (12), and its applicability to recent estuarine sediments in the Solent area is discussed by Cundy (10).

The <sup>137</sup>Cs activity vs depth profile in Figure 2 shows two main peaks. Using <sup>210</sup>Pb and <sup>60</sup>Co dating, it is clear that this pattern cannot be interpreted simply and is inconsistent with the other dating evidence. Instead, the accumulation rates calculated from <sup>60</sup>Co and <sup>210</sup>Pb distributions are used to determine the <sup>137</sup>Cs flux (Figure 3; decay corrected), and the result shows that there is only a single broad peak. The upper peak in the activity profile (Figure 2) is therefore a result of the much lower accumulation rate occurring from the late-1960s onward.

Heavy Metals. (A) Copper. The profile obtained for copper is shown in Figure 2, and raw data are shown in Table 2. The copper profile shows a rapid increase from background levels of 15 ppm at 43 cm depth, coinciding with the observed changes in color and compaction of the sediment following the expansion of the Fawley refinery. The Fawley oil refinery is the main contributor of copper into Southampton Water (7, 8). Highly elevated concentrations of up to 1022 ppm in the sediments are observed with a decrease in recent years to 286 ppm presumably caused by more efficient cleanup of effluent (4, 7). Average copper concentrations in the sediment before and after refinery expansion are shown in Table 3 and compared with copper values from the non-industrialised Newtown estuary, Isle of Wight (averaged over the same time period, data from ref 10). The background copper concentrations prior to large-scale refinery output compare well with the 15–22 ppm reported by Ármannsson (11) and Sharifi (8). The maximum copper concentrations are over 50 times the background level and over an order of magnitude higher than those observed at Newtown. The biological effects of this copper enrichment (and hydrocarbons) have been discussed by Knap (4), Dicks and Levell (7), and Sharifi (8). The onset of elevated copper concentrations can be linked to the expansion of the refinery and so can be used to provide a measure of sediment accretion over the period 1949–1951 through 1989, giving an average accumulation

TABLE 2

Geochemical Data, Fawley Core<sup>a</sup>

Section A: Fawley Subtidal Core																			
sample depth (cm)	FW1 -3	FW2 -6	FW3 -9	FW4 -12.5	FW5 -16	FW6 -19	FW7 -22	FW8 -25	FW9 -28	FW10 -31	FW11 -34	FW12 -37	FW13 -40	FW14 -43	FW15 -46	FW16 -49	FW17 -52	FW18 -55	
major elements (wt %)																			
SiO <sub>2</sub>	54.89	56.48	56.88		56.25	55.32	53.90	53.57	53.25	52.32	54.46	53.41	53.52	53.47	56.04	55.30	55.73	54.02	
TiO <sub>2</sub>	0.80	0.80	0.80	0.78	0.81	0.78	0.78	0.74	0.77	0.76	0.79	0.76	0.78	0.77	0.75	0.75	0.77	0.76	
Al <sub>2</sub> O <sub>3</sub>	13.27	12.51	12.54		10.61	11.48	12.10	12.84	13.01	12.91	12.80	13.14	13.28	12.56	11.34	11.58	11.76	12.20	
Fe <sub>2</sub> O <sub>3</sub>	5.84	5.94	5.76		4.97	5.18	5.19	5.55	5.76	5.31	5.53	5.97	6.02	5.59	5.14	5.24	5.20	5.22	
MnO	0.03	0.04	0.03	0.04	0.04	0.03	0.03	0.03	0.03	0.03	0.03	0.03	0.03	0.04	0.04	0.03	0.04	0.04	
MgO	1.70	1.57	1.55		1.52	1.55	1.56	1.66	1.68	1.64	1.68	1.69	1.72	1.61	1.43	1.44	1.43	1.50	
CaO	1.37	1.87	2.02		4.43	4.02	2.90	2.14	2.39	2.86	3.00	3.09	2.54	4.23	5.88	6.14	6.33	6.97	
Na <sub>2</sub> O	2.70	2.21	2.20		2.16	2.36	2.43	2.65	2.69	2.64	2.69	2.81	2.75	2.24	1.72	1.69	1.58	1.71	
K <sub>2</sub> O	2.45	2.28	2.39		2.09	2.08	2.25	2.34	2.35	2.36	2.36	2.26	2.40	2.30	2.17	2.21	2.19	2.22	
P <sub>2</sub> O <sub>5</sub>	0.17	0.17	0.16		0.16	0.17	0.17	0.17	0.17	0.17	0.17	0.17	0.18	0.16	0.14	0.14	0.13	0.14	
LOI	16.8	16.2	15.7		17.0	17.0	18.7	18.3	17.9	19.0	16.5	16.7	16.8	17.1	15.4	15.5	14.9	15.3	
S	1.84	2.02	2.23		1.75	1.49	1.48	1.73	1.75	1.53	1.57	1.41	1.48	1.36	1.73	1.63	1.77	1.59	
Cl	0.93	0.66	0.68		0.67	0.72	0.72	0.76	0.76	0.74	0.75	0.75	0.74	0.72	0.63	0.48	0.42	0.36	
trace elements (ppm)																			
Br	197	168	155	141	134	159	173	183	187	188	181	193	192	159	115	105	96	103	
I	42	35	35	23	22	30	35	36	34	39	38	41	37	35	25	23	21	18	
Pb	67	65	59	61	68	93	109	109	91	86	84	83	79	70	25	22	23	26	
Zn	161	168	169	153	126	127	141	154	147	144	136	142	146	129	75	73	73	77	
Ni	34	34	35	30	28	30	33	33	36	32	31	31	32	32	26	25	25	27	
Cr	102	102	98	90	96	95	93	92	98	97	92	93	95	89	87	88	87	88	
V	143	138	136	128	115	115	132	144	146	147	143	147	151	138	125	129	132	128	
As	18	16	17	18	16	13	15	24	19	19	15	16	18	31	12	17	12	11	
Cu	286	475	711	963	692	768	991	1022	424	277	218	206	211	110	15	12	11	20	
radionuclide data (Bq/kg)																			
Cs-137	18	16	19	17	11	9	9	10	6	0	0	0	0	0	0	0	0	0	
Co-60	28	19	7	1	0	0	0	0	0	0	0	0	0	0	0	0	0	0	
Po-210 total	33	29	24	20	19	22	24	23	22	24	22	23	21	20	12	11	11	12	
Po-210 sup	11	11	11	11	11	11	11	11	11	11	11	11	11	11	11	11	11	11	
Po-210 xs	22	18	13	9	8	11	13	12	11	13	11	12	10	9	1	0	0	1	
Pb isotope ratios																			
Pb-206/Pb-207		1.138			1.133		1.125			1.140	1.131		1.137	1.137	1.175				1.180
Pb-206/Pb-208		0.470			0.471		0.476			0.473	0.471		0.473	0.473	0.480				0.480

# Section B: Newtown Intertidal Core

sample depth (cm)	NT/1	NT/2	NT/3	NT/4	NT/5	NT/6	NT/7	NT/8	NT/9	NT/10	NT/11	NT/12	NT/13	NT/14	NT/15	NT/16
major elements (wt %)	-1	-3	-5	-7	-9	-11	-13	-15	-17	-19	-21	-23	-25	-27	-29	-31
SiO <sub>2</sub>	56.80	64.35	71.44	64.95	66.33	65.63	66.51	67.87	67.92	66.75	68.41	63.73	61.37	59.65	58.14	53.60
TiO <sub>2</sub>	0.76	0.68	0.58	0.68	0.77	0.78	0.79	0.77	0.81	0.76	0.77	0.80	0.84	0.84	0.84	0.89
Al <sub>2</sub> O <sub>3</sub>	11.08	8.10	6.34	7.80	9.05	9.12	9.02	9.25	9.28	9.19	8.92	10.44	11.97	11.88	13.18	15.66
Fe <sub>2</sub> O <sub>3</sub>	4.93	4.84	4.64	5.66	5.69	6.52	6.28	5.80	5.85	6.14	6.27	6.14	6.31	6.44	6.74	7.04
MnO	0.02	0.02	0.02	0.03	0.03	0.04	0.04	0.04	0.03	0.03	0.03	0.04	0.05	0.05	0.05	0.06
MgO	1.34	1.06	0.77	0.94	0.94	0.96	0.93	0.96	0.95	0.94	0.91	1.10	1.25	1.28	1.40	1.68
CaO	2.33	1.93	1.36	1.64	1.42	1.36	1.27	1.31	1.16	1.12	1.09	1.13	1.03	1.00	1.00	0.97
K <sub>2</sub> O	2.11	1.60	1.25	1.54	1.75	1.77	1.74	1.81	1.82	1.80	1.76	2.09	2.43	2.48	2.74	3.27
P <sub>2</sub> O <sub>5</sub>	0.21	0.16	0.13	0.13	0.12	0.13	0.13	0.14	0.12	0.12	0.14	0.13	0.14	0.14	0.14	0.15
LOI	19.5	16.8	13.0	16.1	13.1	12.7	12.2	10.9	10.9	12.0	10.7	12.6	11.8	12.5	12.4	11.9
S	0.92	1.66	1.92	2.68	2.18	2.10	1.98	1.63	1.63	1.90	1.54	1.20	0.79	0.74	0.50	0.11
Cl	1.05	1.10	0.96	0.92	0.68	0.60	0.60	0.56	0.51	0.51	0.50	0.49	0.36	0.34	0.28	0.25
trace elements (ppm)																
Br	341	266	172	151	105	97	82	78	75	76	73	69	55	52	45	32
I	79	53	33	22	13	13	12	11	8	12	9	10	6	9	7	2
Pb	61	48	34		35	33	32	31	31	27	27	37	30	30	30	33
Zn	99	91	75	81	76	77	73	72	73	71	73	81	84	83	88	93
Ni	31	30	28	30	30	31	28	29	30	29	30	33	38	39	44	44
Cr	78	76	65	71	77	81	84	71	89	82	79	86	88	84	80	92
V	129	115	98	109	112	113	109	110	109	105	113	115	124	120	126	133
As	20	20	18	22	16	13	12	14	9	13	13	11	13	6	9	3
Cu	24	22	18	16	16	16	16	16	15	14	16	17	19	18	21	23
radionuclide data (Bq/kg)																
Cs-137	12	10	8	6	2	2	0	0								
Co-60	17	18	12	6	0	0	0	0								
Po-210 total	38	30	30	14	11	12	12	12	11	12	11	13	14	13	14	
Po-210 sup	12	12	12	12	12	12	12	12	12	12	12	12	12	12	12	
Po-210 xs	26	18	18	2	-1	0	0	0	-1	0	-1	1	2	1	2	

<sup>a</sup> Data from an intertidal mudflat core taken from the Newtown Estuary, Isle of Wight, are also shown to enable comparison with (relatively) unpolluted sediment.

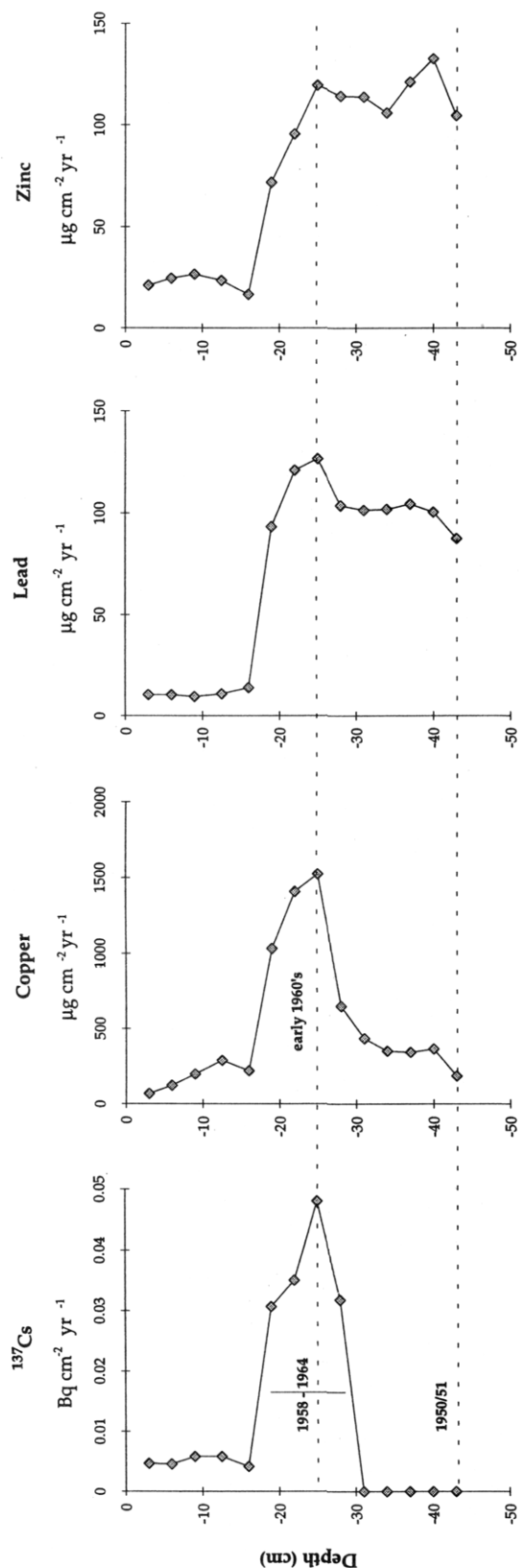


FIGURE 3. Annual flux of  $^{137}\text{Cs}$ , copper, lead, and zinc to sediments around the sampling site. Fluxes are calculated using the equation  $\text{flux} = \text{concentration} \times \rho \times \text{sediment accumulation rate}$ . Density data are from ref 10.

rate of 11 mm p.a. over this 40-year period (Table 1).

**(B) Lead and Pb Isotope Ratios.** While the main anthropogenic source of copper into Southampton Water has been identified as the Fawley refinery, lead may have a number of different sources. Lead isotope ratios have been used by a number of researchers to determine historical sources of lead pollution (e.g., ref 16) and in the Solent estuarine system by Cundy (10). Lead present in marine sediments is a mixture of the inherent mineral lead and anthropogenic lead inputs derived from sources such as automobile emissions (17), industrial uses (e.g., ship-building), and fly ash from coal burning. In general, petroleum alkyl lead and industrial lead are derived mainly from Precambrian lead ores, most probably imported from Canada and Australia. This could be mixed with varying amounts of younger lead from the United States, but these younger sources have only contributed in recent years (18). Each source generally has its own distinctive Pb isotope signature, and the measured Pb isotopic abundance is a mix of these source terms proportionately weighted according to their input.

Figure 2 shows total lead,  $^{206}/^{207}\text{Pb}$ , and  $^{206}/^{208}\text{Pb}$  for the Fawley core. As for copper, lead shows an increase from a background concentration of approximately  $24 \pm 4$  ppm to a maximum of 109 ppm at 22–25 cm depth, followed by a slight decrease toward the surface. Below 42.5 cm depth the  $^{206}/^{207}\text{Pb}$  and  $^{206}/^{208}\text{Pb}$  ratios are from pre-/early Industrial Holocene sediments and have values of 1.18 and 0.48, respectively. In sediment deposited after refinery expansion the isotopic ratios are significantly lower, due to mixing of the inherent mineral lead with anthropogenic lead originating from various sources. Figure 4 highlights this mixing effect where the pre-/early Industrial Holocene sediment (below 43 cm depth) has a lead isotopic composition similar to coal, whereas the values for sediment deposited after refinery expansion fall on a mixing line between those of the pre-/early Industrial Holocene sediments and Precambrian lead end members. Mass balance calculations suggest that the higher postrefinery lead concentrations are due to a mixing of background lead with a pollution source having a significantly lower  $^{206}/^{207}\text{Pb}$  ratio, consistent with industrial use of Precambrian Australian/Canadian ores. The peak in lead concentration at 22–25 cm depth (Figure 2) is caused by an increased input of this low ratio lead rather than an input of lead from a different source. The refinery is a possible source for this lead, through discharge of alkyllead derivatives and its use of Pb elsewhere in the plant. The lead peak at 22–25 cm depth is coincident with peak copper concentrations, suggesting that a peak discharge of refinery effluent occurred in the early 1960s. Industrial effluent from several possible plants are likely. It is notable that the Pb content of a hydrocarbon extract from the core was so low as to be unmeasurable by ICP/MS. Car exhaust emissions, particularly prior to 1980, contain alkyl lead derivatives manufactured using mainly ancient ores with varying amounts of U.S.-derived, younger lead (Associated Octel, personal communication). If this were the major source of the ancient lead however, one would expect to see a progressive decrease in  $^{206}/^{207}\text{Pb}$  due to increasing vehicle densities around Southampton from 1950 onward rather than the pattern observed.

**(C) Zinc.** Zinc shows a similar distribution to lead, although there is an increase in its concentration toward the top of the core. The source of zinc is uncertain, but its elevated level compared with sediments from the unpol-

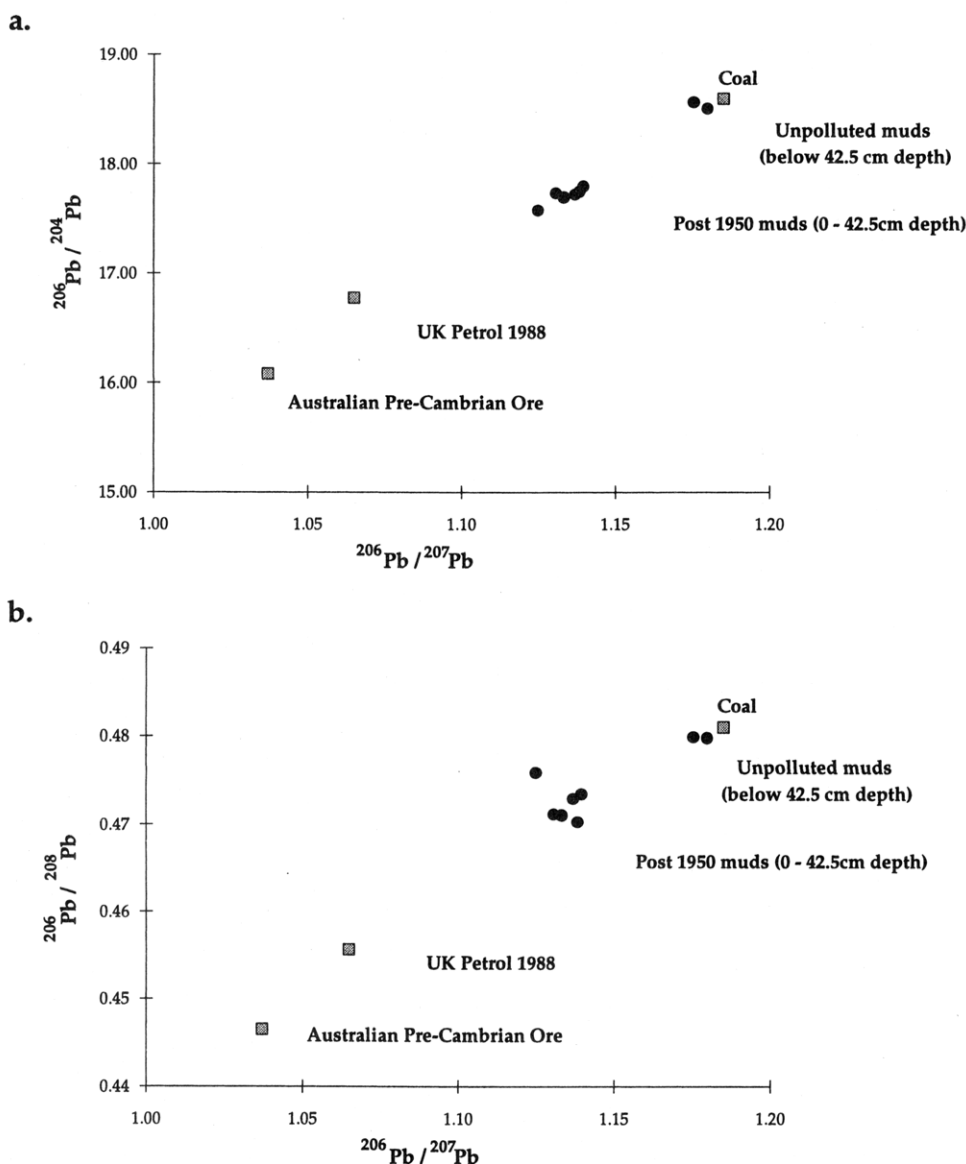


FIGURE 4.  $^{206}\text{Pb}/^{204}\text{Pb}$  versus  $^{206}\text{Pb}/^{207}\text{Pb}$  and  $^{206}\text{Pb}/^{208}\text{Pb}$  versus  $^{206}\text{Pb}/^{207}\text{Pb}$  for Fawley subtidal core. End-member ratios are from Chow et al. (16) with the following exceptions:  $^{206}\text{Pb}/^{207}\text{Pb}$  petrol value is from ref 19; corresponding petrol ratios are calculated from ref 16, using a ratio of 70:30 Australian:New Brunswick ore mix for the alkyllead additive (17). Coal ratios used are those of North American coal having a similar  $^{206}\text{Pb}/^{207}\text{Pb}$  composition to domestic British coal (16).

TABLE 3

**Mean Copper Concentrations in Newtown and Fawley Sediments for 1950–1989<sup>a</sup>**

location	mean Cu concn in sediment (ppm)
Newtown, Isle of Wight (post-1950)	23 ± 1
Fawley (pre-1950)	15 ± 4
Fawley (post-1950)	525 ± 325 (1022) <sup>b</sup>

<sup>a</sup> A pre-1950 mean is shown for Fawley as a pre/early Industrial value.

<sup>b</sup> Maximum value is given in parentheses.

luted Newtown Estuary suggests an anthropogenic input. Other trace and major element data are shown in Table 2.

**Cu, Pb, and Zn Fluxes.** Figure 3 shows the annual flux of copper, lead, and zinc to sediments around the sampling area, calculated using the sediment accumulation rates derived in the previous sections. Prior to calculation, the inherent metal concentration of the sediment was subtracted. This is taken as approximate to the concentration

in the unpolluted lowermost clay, which is also similar to concentrations in sediment cores collected from relatively unpolluted estuaries. The profiles indicate that the maximum flux of copper and lead to the estuary occurred in the early 1960s, with a much reduced flux over the last 20 years. The flux data indicate that the double peak pattern observed for copper, when looking at concentration data alone, is due to variation in sediment accumulation rate rather than variation in the amount of copper discharged from the refinery. A similar decline in flux over the last 20 years is indicated for zinc, suggesting that the general increase in zinc concentration at the top of the core is an artifact of the decreasing sediment accumulation rate. The data show the importance of using flux rather than concentration data for pollution impact studies.

**Summary: Influence of Industrialization on Sedimentation Regime.** The sediment accumulation rates given in Table 1 show an initially higher sediment accretion rate of 20 mm p.a. immediately after the expansion of the Fawley oil refinery. This then decreases with time to an



average rate of less than 5 mm p.a. between 1981 and 1989. The rapid drop to background levels for copper and the lack of  $^{210}\text{Pb}_{\text{XS}}$  below 42.5 cm indicate that the area was dredged immediately prior to the expansion of the refinery, removing the Holocene layers of sediment and exposing the pre/early Industrial Holocene beds. The initial more rapid sedimentation following the refinery expansion is presumably due to an increase in suspended solid matter and also to readjustment of the hydrographic circulation and sedimentary regime to the new, overdeepened, bed conditions. The element flux data are particularly interesting and indicate that there has been a notable decline in the amount of copper, lead, and zinc introduced into the estuary in the last 20 years. The data graphically demonstrate the misleading impression that may be gained from looking at concentration data alone.

## Conclusions

A sediment core retrieved from the Fawley area of Southampton Water reveals a clear record of anthropogenic inputs. A combination of heavy metal analyses, the first appearance of hydrocarbon contamination, radiometric dating, and stable Pb isotope ratios are used to interpret the pollution history in the core. The main source of pollution is from the oil refinery at Fawley, developed from 1949–1951 onward, discharging hydrocarbon pollution and elevated copper concentrations. Dating of the sediment core using five independent methods reveals that the cored area was dredged prior to refinery expansion, after which a period of initially rapid sediment accumulation began. This has decreased significantly with time. As for copper, post-1950 lead and zinc in the sediment shows a marked enrichment over background levels. Elemental flux data are presented to reveal the real character of element input into the Fawley area which have a different form from the simple concentration profiles. Lead isotope ratios indicate a significant “ancient” (anthropogenic) lead component in sediment deposited after refinery expansion, containing lead originating mainly from the use of Precambrian ores.

## Acknowledgments

A.B.C. is grateful to the University of Southampton Advanced Studies Committee for the award of a Research Studentship. We thank John Thomson of IOSDL for providing a constructively critical review of an early draft of the paper, Bob Nesbitt for the use of the Fisons Elemental Plasmaquad PQ2 (EEC BRITE-EURAM Grant), and Tak Hirata for his considerable technical expertise and valuable assistance. Rahim Sharifi generously provided the core for

investigation. Finally, John Murray is thanked for making a foraminiferal examination of the lowermost part of the core.

## Literature Cited

- (1) Dyer, K. R. *Estuaries: A physical introduction*; Wiley: London, 1973.
- (2) Macmillan, D. H. The hydrography of the Solent and Southampton Water. In *A survey of Southampton and its region*; Monkhouse, F. J., Ed.; British Association for the Advancement of Science: London, 1964; pp 51–65.
- (3) Webber, N. B. Hydrology and water circulation in the Solent. In *The Solent estuarine system—an assessment of present knowledge*; NERC Publication Series C22; 1980; pp 25–35.
- (4) Knap, A. H. The fate of non-volatile petroleum hydrocarbons in refinery effluent entering Southampton Water. Ph.D. Dissertation, University of Southampton, 1979.
- (5) Fawley. *Esso Exxon Chemicals*; Public Information Brochure, Public Affairs Department, Esso House, London, 1987.
- (6) Armansson, H.; Burton, J. D.; Jones, G. B.; Knap, A. H. *Mar. Environ. Res.* **1985**, *15*, 31–44.
- (7) Dicks, B.; Levell, D. Refinery-effluent discharges into Milford Haven and Southampton Water. In *Ecological impact of the oil industry*; Dicks, B., Ed.; Wiley: New York, 1989.
- (8) Sharifi, A. R. Heavy metal pollution and its effects on recent foraminiferids from Southampton Water, Southern England. Ph.D. Dissertation, University of Southampton, 1991.
- (9) Flynn, W. W. *Anal. Chim. Acta* **1968**, *43* 221–227.
- (10) Cundy, A. B. Radionuclide and geochemical studies of recent sediments from the Solent estuarine system. Ph.D. Dissertation, University of Southampton, 1994.
- (11) Armansson, H. Analytical geochemical studies on cadmium and some other trace metals in estuarine and coastal environments. Ph.D. Dissertation, University of Southampton, 1979.
- (12) Ritchie, J. C.; McHenry, J. R. *J. Env. Qual.* **1990**, *19* (2), 215–233.
- (13) AEE Winfrith. Annual report on radioactive discharges from Winfrith and monitoring the environment 1992. AEA Technology Report WER-8-1992, 1993.
- (14) Appleby, P. G.; Oldfield, F. Application of  $^{210}\text{Pb}$  to sedimentation studies. In *Uranium-series disequilibrium. Applications to earth, marine and environmental sciences*, 2nd ed.; Ivanovich, M., Harmon, R. S., Eds.; Oxford Science: Oxford, 1992; pp 731–778.
- (15) Robbins, J. A. Geochemical and geophysical applications of radioactive lead. In *The biogeochemistry of lead in the environment, Part A*; Nriagu, J. O., Ed.; Elsevier/North Holland Biomedical Press: Amsterdam, 1978; pp 285–293.
- (16) Chow, T. J.; Snyder, C. B.; Earl, J. L. Isotope ratios of lead as pollutant source indicators. In *Isotope ratios as pollutant source and behaviour indicators*; IAEA: Vienna, 1975; pp 95–108.
- (17) Sugden, C. L.; Farmer, J. G.; MacKenzie, A. B. *Environ. Geochem. Health* **1993**, *15* (2/3), 59–65.
- (18) Hamelin, B.; Grousset, F.; Sholkovitz, E. R. *Geochim. Cosmochim. Acta* **1990**, *54*, 37–47.
- (19) Delves, H. T. *Chem. Brit.* **1988**, *24*, 1009–1012.

Received for review August 8, 1994. Revised manuscript received January 26, 1995. Accepted January 31, 1995.\*

ES9405080

\* Abstract published in *Advance ACS Abstracts*, March 15, 1995.